

# **FATIGUE BEHAVIOUR STUDY OF LASER HYBRID WELDED ECCENTRIC FILLET JOINTS – PART II: STATE-OF-THE-ART OF FRACTURE MECHANICS AND FATIGUE ANALYSIS OF WELDED JOINTS.**

**M. M. Alam, A. F. H. Kaplan, P. Jonsén**

<sup>1)</sup>Luleå University of Technology, Dept. of Applied Physics and Mechanical Engineering, Sweden, [www.ltu.se/tfm/produktion](http://www.ltu.se/tfm/produktion)

## **ABSTRACT**

Simplified fatigue and fracture mechanics based assessment methods are widely used by the industry to determine the structural integrity significance of postulated cracks, manufacturing flaws, service-induced cracking or suspected degradation of engineering components under normal and abnormal service loads. In many cases, welded joints are the regions most likely to contain original fabrication defects or cracks initiating and growing during service operation. The welded joints are a major component that is often blamed for causing a structure failure or for being the point at which fatigue or fracture problems initiate and propagate. Various mathematical models/techniques for various classes of welded joints are developed by analytically or by simulation software's that can be used in fatigue and fracture assessments. This literature survey compiled useful information on fracture and fatigue analysis of various welded joints. The present review is divided into two major sections- fracture mechanics and fatigue analysis with widely used models. A survey table is also introduced to get the outlook of research trend on fatigue and fracture over last 3 decades. Although tremendous research effort has been implemented on fatigue and fracture analysis of conventional welding, research on relatively new welding technology (laser welding, hybrid laser welding) is still limited and unsatisfactory. In order to give guarantee or make welding standard for new welding technology, further research is required in the field of fatigue and fracture mechanics including FEM and multi-scale modeling.

**Keywords:** *fracture mechanics, fatigue, welded joints, welding standards, FEM, multi-scale modeling.*

## **1. INTRODUCTION**

This paper is a literature survey which compiled useful information regarding fracture and fatigue analysis of various welded joints. The main objective was on to analyze fracture mechanics and fatigue life prediction on hybrid laser welded joints. Since hybrid laser

welding is a new technology and very few researches have been done on this area, this literature survey has to restrict on conventional welding process from where fracture and fatigue analysis are shortly presented. Around 550 publications are illustrated in [1]. This paper is mainly divided into two major section- fracture mechanics and fatigue analysis. In fracture mechanics, a basic study on fracture mechanics is given followed by three different approaches on three types welding joints and fatigue analysis section is oriented by four fatigue assessment method from where two methods are described briefly.

Nowadays, the trend is to use the welded structures to the maximum of their life potential. To achieve this aim, considerable effort should be paid on design of welded joints. Weld joints are characterized by differences in mechanical properties produced by geometrical, material and metallurgical discontinuities. The heat-affected zone is usually a source of failure of welded parts/structures. The quality of welding has strong influence on the strength of whole structure beside the welding depth and the geometry of the weld surface. The presence of cracks, defects and residual stresses is a danger to structure in service. To determine residual stresses, cracks, defects, there are several approaches based on fracture mechanics. Two main approaches are mostly used: *Linear Elastic Fracture Mechanics (LEFM)* and *Elastic Plastic Fracture Mechanics (EPFM)* [4]. In this literature survey, these two approaches have been focused on.

A material fractures when sufficient stress and work are applied on the atomic level to break the bonds that hold atoms together. The bond strength is supplied by the attractive forces between atoms. **Figure 1** shows schematic plots of the potential energy and force versus separation distance between atoms.

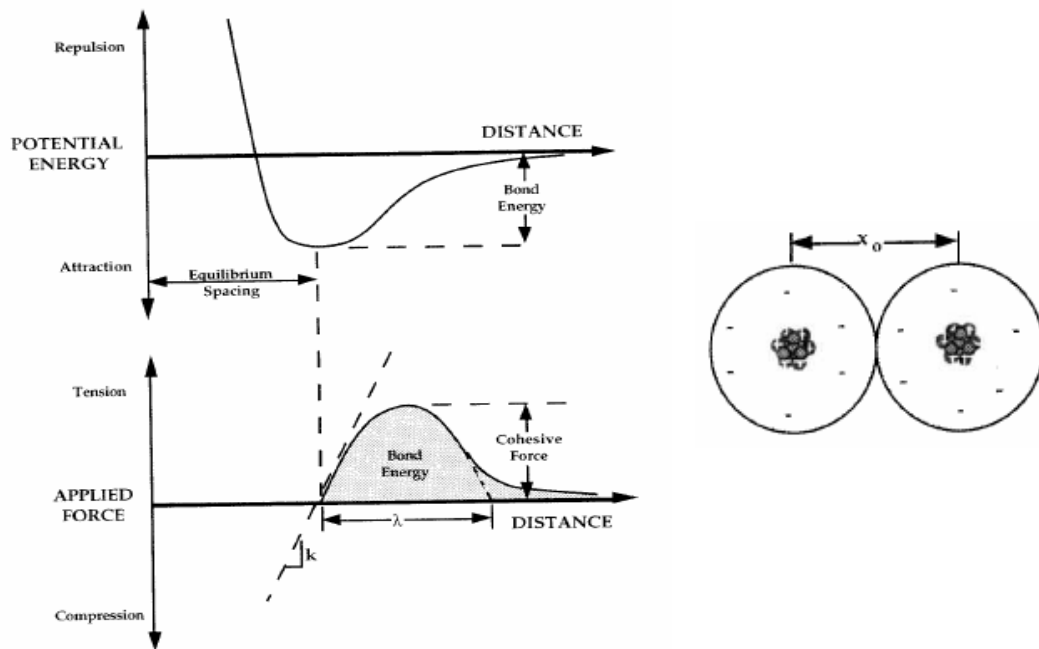


**Fig. 1:** Potential energy and force as a function of atomic separation [4]

The equilibrium spacing occurs where the potential energy is at a minimum. At the equilibrium separation,  $x_0$ , the potential energy is minimized and the attractive and repelling forces are balanced. A tensile force is required to increase the separation distance from the equilibrium value; this force must exceed the cohesive force to sever the bond completely.

Fatigue is a mechanism of failure which involves the formation and growth of cracks under the action of repeated stresses. Ultimately, a crack may propagate to such an extent that total fracture of the member may occur. It is known that the local weld geometry, toe angle, toe radius, undercuts and cracks strongly influence the fatigue strength. The local geometry affects the local stress concentration and together with defects of different types fatigue cracks may form during cyclic loading and lead to large scatter in fatigue life [46]. At present, there are two primary approaches used for predicting fatigue life, namely, the fracture mechanics approach and the S-N curve approach. See **Fig 21**. The relationship between these approaches as depicted in **Fig.2**

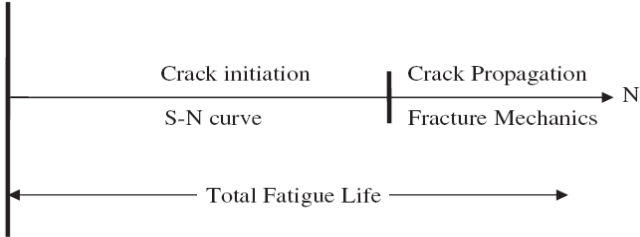


**Fig. 2:** Relationship between the characteristics S-N curve and fracture mechanics approaches [22]

**2. SURVEY OF JOURNALS**

**Table1.** Survey of publications on fracture mechanics and fatigue analysis

| No. | Author name   | Country  | Welding types | Joint types | Critical weld location | Mathematical Models /Techniques | Simulation software | Estimation /Goal                | Year |
|-----|---------------|----------|---------------|-------------|------------------------|---------------------------------|---------------------|---------------------------------|------|
| 7   | B. Chang      | China    | S             | L           |                        | Experimental                    |                     | Hardness distribution           | 1999 |
| 8   | P. Dong       | USA      |               | L,T         | T                      | FEM                             |                     | Structural Stress               | 2001 |
| 9   | El-Sayed      | USA      | S             | S           | T                      | FEM                             | NA                  | Fatigue life estimation         | 1996 |
| 10  | H.F.Henrysson | Sweden   | S             | S           | T                      | Coarse FEM                      |                     | Fatigue life prediction         | 2000 |
| 11  | H.Remes       | Finland  | L             | B           | R                      | Theoretical                     |                     | Fatigue strength                | 2003 |
| 12  | S.K.Cho       | S. Korea | L             | T           | T                      | Thermo-elastic-plastic FEM      | AB                  | Fatigue strength                | 2003 |
| 13  | S.J.Maddox    | UK       |               | C           | T                      | Fracture mechanics              |                     | Fatigue cracks                  | 1973 |
| 14  | M.S.Alam      | USA      |               | B           | T                      | FEM                             | AN                  | Simulation-fatigue crack growth | 2004 |
| 15  | L.S.Etube     | UK       |               | U           |                        | Statistical                     |                     | Y correction factor             | 2000 |
| 16  | M.A.Sutton    | Columbia | F             | B           |                        | FEM                             | AN                  | Residual stress                 | 2006 |

|    |                |             |   |     |      |                                |    |   |      |
|----|----------------|-------------|---|-----|------|--------------------------------|----|---|------|
| 17 | B.Guha         | India       | F | C   | R    | Strain Energy density approach |    | Crack growth behavior                               | 1999 |
| 18 | P.J.Haagensen  | Norway      | T | L,T | R    | Ultrasonic impact treatment    |    | Introduction of fatigue test                        | 1998 |
| 19 | T.L.Teng       | Taiwan      | T | B   | T    | Strain based                   |    | Prediction-fatigue crack initiation                 | 2003 |
| 20 | X.Y.Li         | Finland     |   | T   | T    | LEFM                           |    | Fatigue strength                                    | 2001 |
| 21 | Y. Jiang       | USA         |   |     |      | Elastic-Plastic                | AB | Crack growth rate and crack direction.              | 2006 |
| 22 | V.Caccese      | USA         | L | C   | T    | Conventional FEM               | AN | Weld geometric profile                              | 2006 |
| 23 | Chris Hsu      | USA         | L | L   | T    | Cyclic stress-strain           |    | Joint stress calculation                            | 1991 |
| 24 | Z.Barsoum      | Sweden      | H | C   | T    | LEFM                           | AN | Fatigue assessment                                  | 2005 |
| 25 | G.Pettersson   | Sweden      |   |     |      | LEFM                           | AN | Non-linear effects                                  | 2004 |
| 26 | P.Andersson    | Sweden      |   | X   |      | Creep ductility-based damage   | AB | Creep crack growth investigation                    | 1999 |
| 27 | A. Assire      | France      |   | X   |      | FEM                            |    | Creep crack initiation and creep growth assessments | 2000 |
| 28 | Y.C.Hou        | USA         |   |     | C    | J-Integral                     |    | Fracture parameter                                  | 1998 |
| 29 | Infante, V     | Portugal    |   | T   | T    | Elastic-Plastic                | AB | Residual Stress analysis                            | 2002 |
| 30 | J..M. Ferreira | Portugal    | A | T,C | T, M | FEM                            |    | Fatigue life prediction                             | 1994 |
| 31 | G.Cam          | Turkey      | L | B   | R    | Experimental                   |    | Mechanical & fracture properties                    | 1999 |
| 32 | B.Atzori       | Italy       |   | C   | T    | LEFM                           |    | Fatigue strength                                    | 1998 |
| 33 | P.J.Budden     | UK          |   |     | C    | Fracture mechanics             | BE | Creep crack growth                                  | 1999 |
| 34 | P.C. Wang      | USA         | L | T   |      | J- Integral                    | AB | Fracture mechanics parameter                        | 1994 |
| 35 | C.Maosheng     | China       | A | B   | T    | Fracture mechanics             |    | Crack growth & fatigue life estimation              | 1990 |
| 36 | H.P.Lieurade   | France      | A | B,C | T    | Fracture mechanics             |    | Fatigue life estimation                             | 1983 |
| 37 | J.C. Newman    | USA         |   |     |      | Weight function                |    | Stress intensity factor                             | 1996 |
| 38 | H.J.Schindler  | Switzerland |   | T,B | R    | LEFM                           |    | Fatigue endurance                                   | 2006 |
| 39 | Chang K.H.     | Korea       | A | B   | C    | Elastic-Plastic                |    | Residual stress                                     | 2006 |
| 40 | Y.Lei          | UK          |   |     | C    | J- Integral                    | AB | Residual stress                                     | 2000 |

|    |            |         |   |     |   |                 |    |                          |      |
|----|------------|---------|---|-----|---|-----------------|----|--------------------------|------|
| 41 | H.Y.Lee    | S.Korea |   | T,B |   | LEFM            | AB | Stress intensity factor  | 2005 |
| 42 | W.Muller   | Germany |   |     | C | Elastic-Plastic | AD | Weld material properties | 1988 |
| 43 | W.Dahl     | Germany | A | T   | C | Elastic-Plastic | AB | Fracture mechanics       | 1986 |
| 44 | M. Chiesa  | Norway  | A |     | C | J-Integral      | AB | Fracture analysis        | 2000 |
| 45 | T. Nykänen | Finland |   | T,B | T | LEFM            | FR | Fracture mechanics study | 2005 |

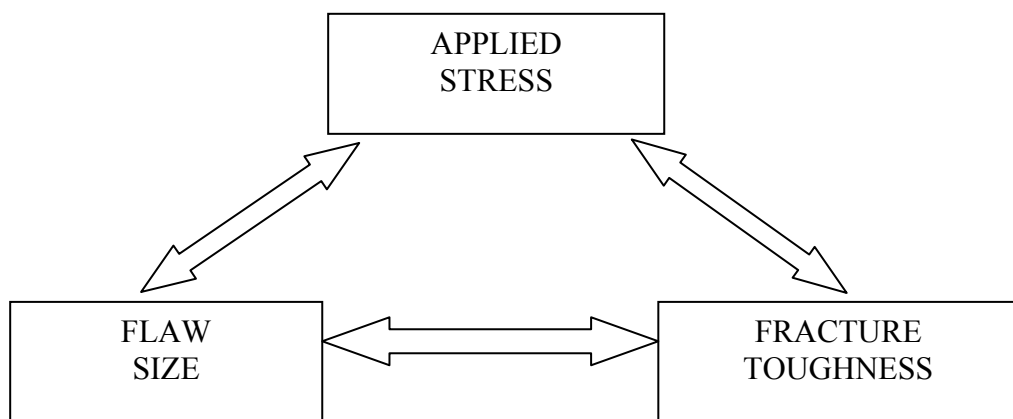
**LEGEND:**

| <b>Joint Type</b> | <b>Welding type</b> | <b>Critical Location</b> | <b>Simulation Software</b> |
|-------------------|---------------------|--------------------------|----------------------------|
| L : Lap           | S : Spot            | T : Toe                  | AB : ABAQUS                |
| T : T             | L : Laser           | R : Root                 | AN : ANSYS                 |
| S : Spot          | F : Friction Stir   | C : Crack tip            | BS : BERSAFE               |
| B : Butt          | A : Arc             | M : Mid. of weld         | FR : FRANC 2D              |
| C : Cruciform     | T : TIG             |                          | NA : NASTRAN               |
| U: Tubular        | H : Hybrid Laser    |                          | AD : ADINA                 |
| X : Cross Weld    |                     |                          |                            |
| F : Fillet        |                     |                          |                            |

**3. FRACTURE ANALYSIS**

**3.1 FUNDAMENTAL KNOWLEDGE ON FRACTURE MECHANICS**

Fracture mechanics is the study of mechanical behaviour of cracked materials subjected to an applied load. Crack growth behavior due to fatigue, stress corrosion, creep, or some combination thereof can be simulated and predicted with the appropriate software and experimental data. [49].The fracture mechanics approach has three important variables:

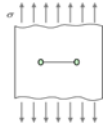
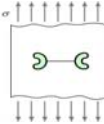


**Fig. 3:** The fracture mechanics approach

Fracture mechanics can be approached from a number of points of view, including energy to cause failure, stress analysis, micro mechanisms of fracture, applications of fracture,

computational approaches and so on. A simplified table for the analysis of fracture mechanics depending on the material properties on fracture shows below:

**Table 2:** Simplified table for the field of fracture mechanics [2]

| Category                                 | Material Property            | Parameter  | Effective Regime  |
|--|------------------------------|--|---|
| Linear Elastic Fracture Mechanics (LEFM) | Linear, time-independent     | Stress intensity factor(K), Energy release rate(G) |  |
| Elastic Plastic Fracture Mechanics       | Non-linear, time-independent | J- Integral, Crack tip opening displacement (CTOD) |  |

### 3.1.1 LINEAR ELASTIC FRACTURE MECHANICS

Linear Elastic Fracture Mechanics (LEFM) first assumes that the material is isotropic and linear elastic. Based on the assumption, the stress field near the crack tip is calculated using the theory of elasticity. When the stresses near the crack tip exceed the material fracture toughness, the crack will grow.

#### THE GRIFFITH ENERGY BALANCE

According to the First Law of Thermodynamics, when a system goes from a non equilibrium state to equilibrium, there will be a net decrease in energy. In 1920 Griffith applied this idea to the formation of a crack. Griffith observed that the strain energy in a body is partly released by the propagation of a crack. At the same time, new surfaces are created in the body, which are associated with a certain surface energy, which in turn is characteristic for a material. According to Griffith, a necessary condition for failure is that the released strain energy, corresponding to a certain crack growth, is greater than the consumed surface energy.

Griffith considered a plane plate of a linear elastic material with a through-thickness crack of length  $2a$ , **Fig. 4**. The in-plane dimensions of the plate are much larger than the length of the crack and in the theory the plate is assumed to be infinite. The boundary of the plate is subjected to a constant and uni-axial stress  $\sigma$  perpendicular to the plane of the crack.

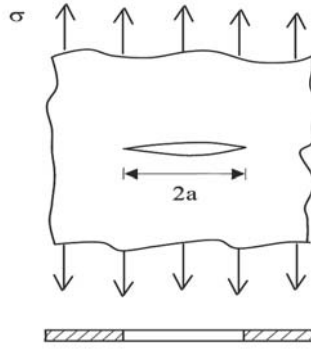


**Fig. 4:** The Griffith crack [4].

From the stress state in a plate with an elliptic hole (Inglis, 1913), Griffith determined the elastic strain energy  $U(a)$  as a function of crack length for a plate with crack:

$$U(a) = U_0 - \frac{\pi\sigma^2 a^2}{E} \quad (1)$$

Where  $U_0$  is the strain energy in the plate without regard to the crack,  $\sigma$  the nominal stress in the crack plane and  $E$  is Young's modulus.

Through crack growth, material close to the newly formed crack surfaces is unloaded and the corresponding elastic energy released. The energy released per unit length of crack growth at a crack tip, or the *crack extension force*  $G$ , is:

$$G = -\frac{dU(a)}{da} = \frac{\pi\sigma^2 a^2}{E} \quad (2)$$

In the crack propagation process, energy is required to create new crack surfaces and for plastic deformation and other dissipative processes adjacent to the new surfaces. The energy required per unit crack length is called the *critical crack extension force*  $G_c$

The condition for fracture is then  $G = G_c$

i.e. fracture occurs at a critical value of the crack extension force.

Thus it can be concluded that failure occurs when the stress, crack length and critical crack extension force are related as follows:

$$G_c = \frac{\pi\sigma_c^2 a_c}{E} \quad (3)$$

Here  $\sigma_c$  is the nominal, or critical, stress at fracture and  $a_c$  the critical crack length.

## STRESS INTENSITY FACTOR

While the energy-balance approach provides a great deal of insight to the fracture process, an alternative method that examines the stress state near the tip of a sharp crack directly has proven more useful in engineering practice. A plane plate with a crack can in the general case be loaded in three different ways, in accordance to the nominal stress components  $\sigma_{yy}$ ,  $\tau_{xy}$  and  $\tau_{yz}$  in the plane of the plate. In **Fig. 5** is shown the stress components and the orientation of the coordinates and of the crack. The plane of the crack is situated in the  $xz$ -plane and the crack front is along the  $z$ -axis.

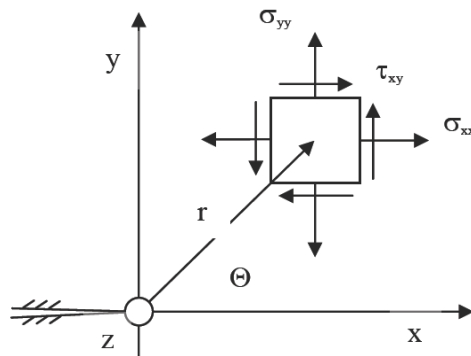


**Fig. 5:** Stress components at a crack tip [4]

Along the  $x$ -axis and ahead of the crack  $\sigma_{yy}$  is the normal stress in the plane of the crack. This stress component tends to open the crack and the corresponding mode of deformation is denoted Mode I.  $\tau_{xy}$  is the shear stress in the plane of the plate and corresponds to in-plane shear, or Mode II deformation. This stress component tends to slide the crack surfaces relative to each other in the plane of the plate.

$\tau_{yz}$  is the shear stress acting perpendicular to the plane of the plate and corresponds to transverse shear, or Mode III deformation. In **Fig. 6** there different crack tip deformation modes are shown: opening, sliding, and tearing:

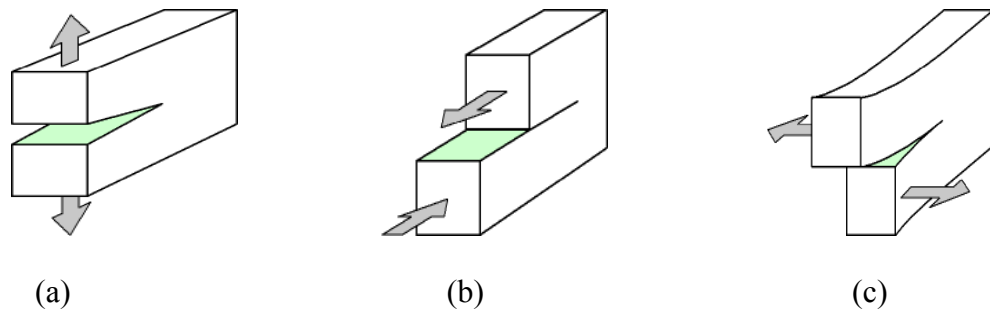


**Fig. 6:** Three basic modes of crack tip deformation. (a) mode I-opening; (b) mode II-sliding; (c) mode III-tearing [2]

In practise Mode I is the most important case and therefore only this mode will be dealt with further here. For Mode I the asymptotic stress field at the tip of a crack in a linear elastic



material is given in the following equation. The origin of the coordinates is located at the crack tip.  $x, y, z$  are Cartesian coordinates and  $r, \theta$  polar coordinates.

$$\begin{aligned}\sigma_{xx} &= \frac{K_I}{\sqrt{2\pi r}} \cos \frac{\theta}{2} \left( 1 - \sin \frac{\theta}{2} \sin \frac{3\theta}{2} \right) \\ \sigma_{yy} &= \frac{K_I}{\sqrt{2\pi r}} \cos \frac{\theta}{2} \left( 1 + \sin \frac{\theta}{2} \sin \frac{3\theta}{2} \right) \\ \tau_{xy} &= \frac{K_I}{\sqrt{2\pi r}} \cos \frac{\theta}{2} \sin \frac{\theta}{2} \cos \frac{3\theta}{2}\end{aligned}\quad (4)$$

In the crack plane  $y = 0$ , where  $r = x$  and  $\theta = 0$  ahead of the crack, (4) reduces to the simpler form:

$$\begin{aligned}\sigma_{xx} = \sigma_{yy} &= \frac{K_I}{\sqrt{2\pi x}} \\ \tau_{xy} &= 0\end{aligned}\quad (5)$$

In (4) all stress components are proportional to the factor  $K_I$ , which accordingly is denoted the *stress intensity factor*.

By applying a virtual crack extension model Irwin (1957) showed that the energy released per unit crack length is:

$$-\frac{dU}{da} = \frac{K_I^2}{E}\quad (6)$$

Eqs. (3) and (6) provides a relation  $G$  and  $K_I$

$$G = \frac{K_I^2}{E}\quad (7)$$

From (3) and (7) the stress intensity factor for the Griffith plate is further obtained as

$$K_I = \sigma \sqrt{\pi a}\quad (8)$$

In practice the general form of the stress intensity factor is

$$K_I = \sigma \sqrt{\pi a} f(g)\quad (9)$$

Where  $f(g)$  is a dimensionless function which depends on the geometry of the cracked body considered.

Expressions for  $K_I$  for some additional geometries are given in Table 3.

**Table 3:** Stress intensity factor for several common geometry

| Type of Crack  | Stress Intensity Factor, $K_I$   |
|--|--|
| Edge crack, length $a$ , in a semi-infinite plate                        | $1.12\sigma\sqrt{\pi a}$   |
| Central penny-shaped crack, radius $a$ , in infinite body                | $2\sigma\sqrt{\frac{a}{\pi}}$  |
| Center crack, length $2a$ in plate of width $W$                          | $\sigma\sqrt{W \tan \frac{\pi a}{W}}$  |
| 2 symmetrical edge cracks, each length $a$ , in plate of total width $W$ | $\sigma\sqrt{W \left[ \tan\left(\frac{\pi a}{W}\right) + 0.1 \sin\left(\frac{2\pi a}{W}\right) \right]}$ |

These stress intensity factors are used in design and analysis by arguing that the material can withstand crack tip stresses up to a critical value of stress intensity, termed  $K_{Ic}$ , beyond which the crack propagates rapidly. *This critical stress intensity factor* is then a measure of material toughness. The failure stress  $\sigma_f$  is then related to the crack length  $a$  and the fracture toughness by

$$\sigma_f = \frac{K_{Ic}}{\alpha\sqrt{\pi a}} \quad (10)$$

where,  $\alpha$  is a geometrical parameter equal to 1 for edge cracks and generally on the order of unity for other situations. Expressions for  $\alpha$  are tabulated for a wide variety of specimen and crack geometries, and specialty finite element methods are available to compute it for new situations.

### 3.1.2 ELASTIC PLASTIC FRACTURE MECHANICS

Elastic Plastic Fracture Mechanics (EPFM) assumes isotropic and elastic-plastic materials. Based on the assumption, the strain energy fields or opening displacement near the crack tips are calculated. When the energy or opening exceeds the critical value, the crack will grow.

For almost all materials, including steel, the engineering stress-strain curve is initially linear, i.e. stress is proportional to strain. A transition to non-linear behavior follows as the material is loaded beyond a limit of proportionality, called the *yield strength* of the material. Within the linear part of the stress-strain curve, deformation is purely *elastic*. If a specimen is unloaded before the yield strength was attained, the unloading curve is identical to the loading curve; see **fig 7 (a)**. After unloading, the specimen returns to its original shape, without any permanent deformation.

A material is said to *flow* when deformed beyond the yield strength. Consider a specimen loaded to the point  $A$  in **Fig. 7(c)** and then unloaded. The unloading will not follow the loading curve backward, but instead a linear curve with the same slope as the initial, elastic curve. The unloading curve is in fact elastic. After unloading a permanent or *plastic* deformation remains in the material. [2]

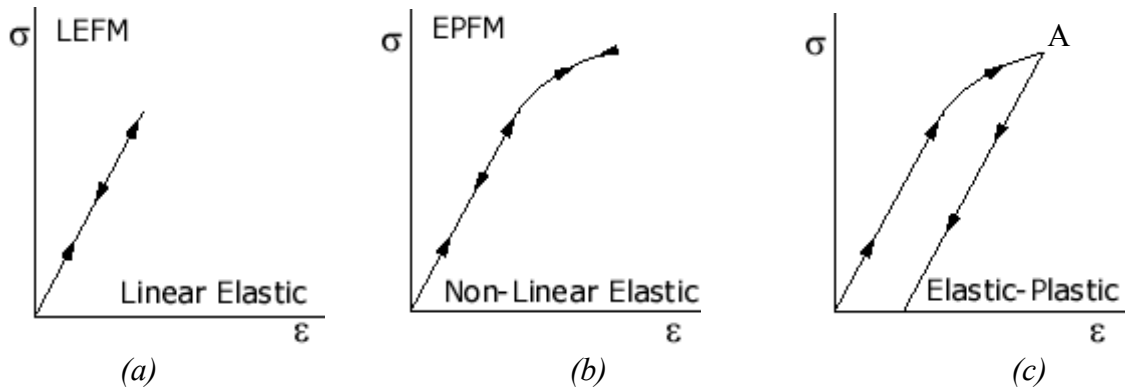


**Fig. 7:** Relationship between LEFM & EPFM. (a) linear elastic curve; (b) non-linear elastic curve; (c) elastic-plastic curve[2]

### NON LINEAR ENERGY RELEASE RATE

In 1956, Irwin proposed an energy approach for fracture. Irwin defined an energy release rate,  $G$ , which is a measure of the energy available for an increment of crack extension:

$$G = -\frac{d\Pi}{dA} \quad (11)$$

where,  $G$  is the rate of change in potential energy with crack area. Equation (11) defines the energy release rate for linear materials. The same definition holds for nonlinear elastic materials except  $G$  is replaced by  $J$ :

$$J = -\frac{d\Pi}{dA} \quad (12)$$

where,  $\Pi$  is the potential energy and  $A$  is crack area. The potential energy is given by

$$\Pi = U - F \quad (13)$$

where,  $U$  is the strain energy stored in the body and  $F$  is the work done by external forces.

Considering a cracked plate which exhibits a nonlinear load-displacement curve, as illustrated in **Fig. 8**

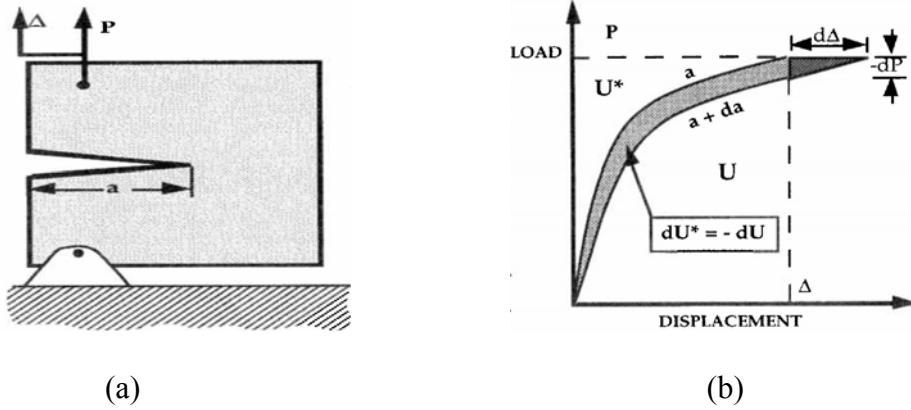


**Fig. 8:** Non-linear energy rate. (a) Cracked plate; (b) Load-displacement curve [4]

In **Fig. 8(b)**, the area under the curve is the strain energy  $U$ , and the area above the curve, called the complementary strain energy,  $U^*$ .

For load control

$$\Pi = U - P\Delta = -U^* \quad (14)$$

where, complementary strain energy is defines as

$$U^* = \int_0^P \Delta dP \quad (15)$$

Thus, if the plate in **Fig. 8 (a)** is in load control,  $J$  is given by

$$J = \left( \frac{dU^*}{da} \right)_P \quad (16)$$

If the crack advances at a fixed displacement,  $F=0$ , and  $J$  is given by

$$J = - \left( \frac{dU^*}{da} \right)_\Delta \quad (17)$$

According to **Fig. 8**,  $dU^*$  for load control differs from  $-dU$  for displacement control by the amount  $\frac{1}{2}dPd\Delta$ , which vanishingly small compared to  $dU$ . There fore,  $J$  for load control is equal to  $J$  for displacement control.

## J INTEGRAL

For a two-dimensional body of area,  $A$ , with surface traction,  $T_i$  prescribed over a portion of the bounding surface,  $\Gamma$ , the potential energy of the body is given by

$$\Pi = \int_A W dA - \int_{\Gamma} T_i u_i ds \quad (18)$$

By differentiating Eqn. 18

$$J = -\frac{d\Pi}{dA} = \frac{1}{B} \int_A \frac{dW}{da} dA - \frac{1}{B} \int_{\Gamma} T_i \frac{du_i}{da} ds \quad (19)$$

After some manipulations, this equation can be written in the form

$$J = \int_{\Gamma} \left( W dy - T_i \frac{\partial u_i}{\partial x} ds \right) \quad (20)$$

Where,  $\Gamma$  is arbitrary counter-clockwise path around crack tip as illustrated in

**Fig.9.**  $W = \int \sigma_{ij} d\varepsilon_{ij}$  is the strain energy density where  $\sigma_{ij}$  is the stress tensor and  $\varepsilon_{ij}$  the strain tensor,  $T_i = \sigma_{ij} n_j$  is the stress vector where  $n_j$  is positive outward unit normal and  $u_i$  the displacement vector and  $ds$  an increment of the length along the path.

$J$  can be evaluated on an arbitrary contour around a crack tip. Because of the property of path independence of the integral, it always yields the same value for any path enclosing the crack tip. Thus  $J$  is called a *path-independent* integral.

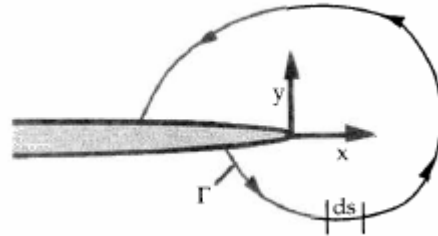


**Fig. 9:** Arbitrary contour around the tip of a crack [4]

## 3.2 WELDED JOINTS ANALYSIS BASED ON FRACTURE MECHANICS

### 3.2.1 T-JOINTS (Stress Intensity approach)

In service cracks may form at the weld toe due to the stress concentration there. Such cracks tend to be along the line A-A in **Fig 10**, i.e. normal to the transverse stress. A fracture assessment for such a crack will generally require the linear elastic stress intensity factor,  $K$ , due to the weld residual stress and any additional primary (mechanical) loading. [3]

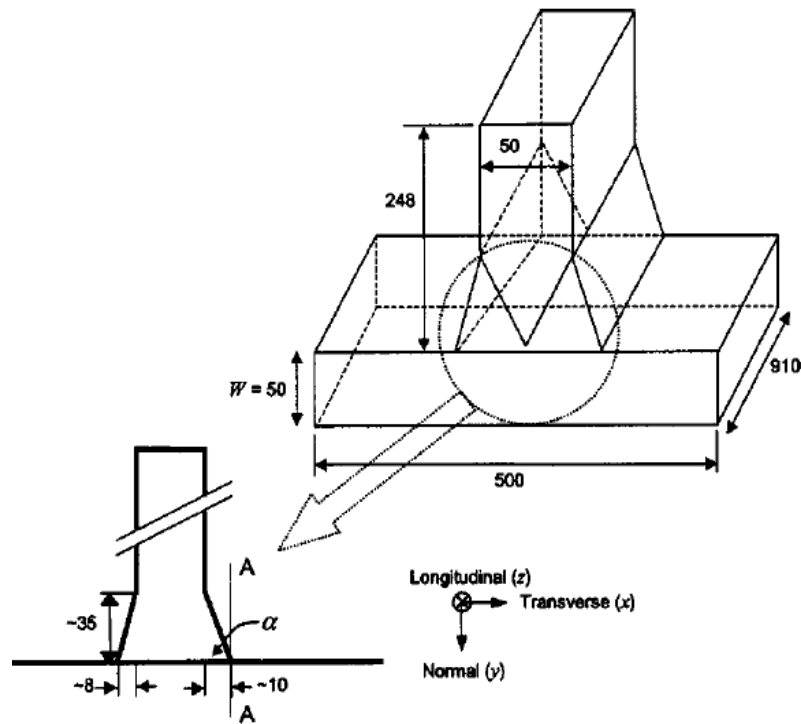


**Fig.10:** Geometry of T-plate weld [3]

The stress intensity factors for the cracked T-plate have been calculated using linear superposition.

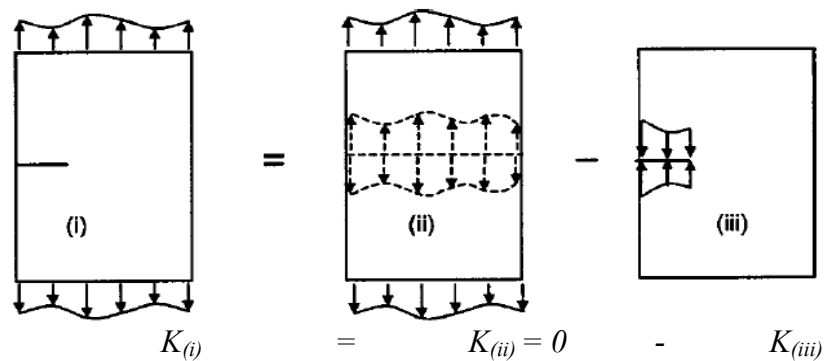


**Fig. 11:** Superposition method to determine stress intensity factor [4]

As illustrated in **Fig.11**, to determine the value of  $K$  only the stress distribution over the crack face is required, i.e.,  $K(i) = -K(iii)$ . For the current problem, the crack face loading is simply the measured (or approximated) residual stress at the weld toe. The approach taken here is analogous to the weight function method, except for the fact that the  $K$  value from the crack face loading is obtained directly using a finite element analysis, rather than by using a weight function.

**FEM Simulation** A typical finite element mesh, which contains 13,000 plane strain four noded elements, is illustrated in **Fig. 12**.

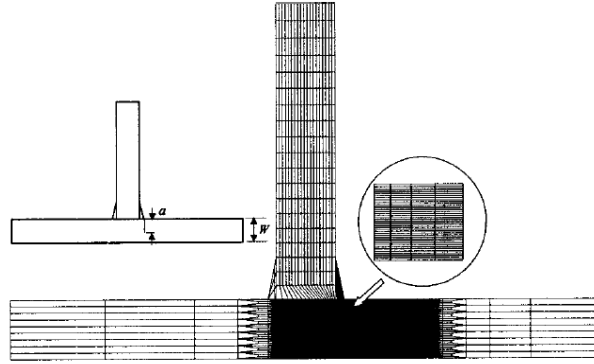


**Fig. 12:** Finite element mesh used in stress intensity factor calculation [3]

The (un-cracked) T-plate is assumed symmetric with weld angle,  $\alpha = 80^\circ$ . A crack of length,  $a$ , is included at the right hand weld toe, as indicated in the inset to **Fig. 7**, thus losing the symmetry of the problem. Because of the very dense mesh near the weld toe the element boundaries are not visible in this region of the figure. The smallest element size is 0.03 mm. The fracture mechanics parameters  $J$  and  $K$  can be calculated from any FEM software— $J$  is calculated using a standard domain integral implementation and  $K$  is obtained using an interaction integral approach. The advantage of the latter approach is that for mixed mode problems, both the mode I and mode II intensity factors,  $K_I$  and  $K_{II}$ , respectively, are calculated. For a mode I linear elastic problem  $K=K_I$  can be evaluated from  $J$  using the relationship (for plane strain),

$$K = \sqrt{\frac{JE}{1-\nu^2}} \quad (21)$$

where  $E$  and  $\nu$  are the Young's modulus and Poisson ratio, respectively.[3]

### 3.2.2 BUTT JOINT (*J-Integral*)

A finite element analysis method which can calculate the J-integral for a crack in a residual stress field is developed to evaluate the J-integral for a centre crack when mechanical stresses were applied in conjunction with residual stresses. In this case, double 'V' butt joint configuration has been showed for joining the plates in **Fig. 13**.

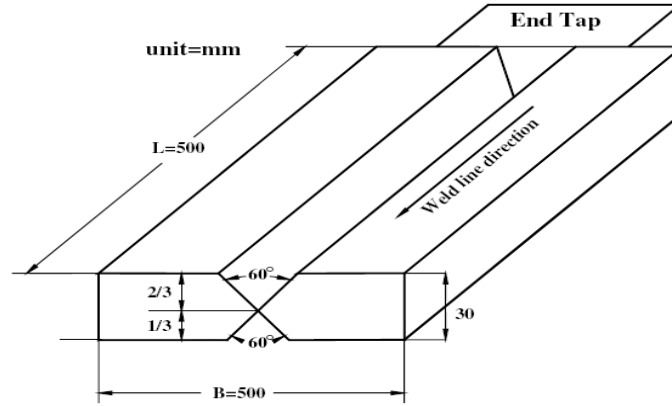


**Fig. 13:** Joint configuration [39]

The J-integral has emerged over the last years as one of the leading parameters to characterize crack-propagation in solids. The J-integral derived by Rice was proposed as the strain energy release rate at the crack tip in linear or nonlinear solid and written as

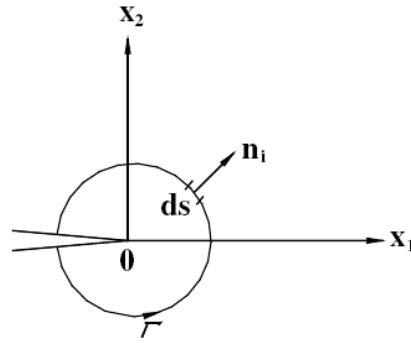


**Fig. 14:** Typical contour for evaluation of J-integral [40]

$$J = -\frac{d\Pi}{da} = \int_{\Gamma} \left( W\delta_{li} - \sigma_{ij} \frac{\partial u_j}{\partial x_1} \right) n_i ds \quad (22)$$

where  $\Pi$  is the potential energy,  $\sigma_{ij}$  and  $u_j$  are components stress and displacement in Cartesian coordinate respectively,  $\Gamma$  is a curve surrounding the crack tip which begins at the lower face of the crack and ends at the upper one,  $n_j$  is the unit vector normal to  $\Gamma$  and  $ds$  is the path length along  $\Gamma$  (**Fig. 14**) and  $W$  is the strain energy density and defined as

$$W = \int_0^{\varepsilon_{ij}} \sigma_{ij} d\varepsilon_{ij}^m \quad (23)$$

### **The J-Integral in a three-dimensional residual stress field**

By applying the divergence theorem to above J-Integral equation and generalizing the results for three dimensions subject to in plane displacement yields



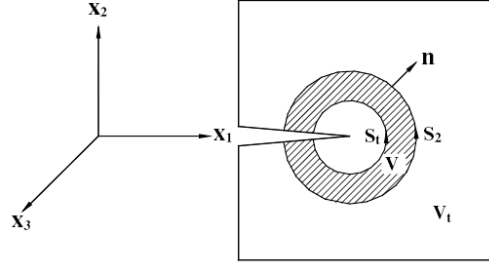


**Fig.15:** Volume  $V$  formed by  $S_t$  &  $S_2$  [40]

$$(J)_{volume} = -\int_v \left( W \frac{\partial q}{\partial x_1} - \sigma_{ij} \frac{\partial u_i}{\partial x_1} \frac{\partial q}{\partial x_j} \right) dV - \int_v \frac{\partial W}{\partial x_1} - \sigma_{ij} \frac{\partial \varepsilon_{ij}^m}{\partial x_1} \quad (24)$$

where,

$$\frac{\partial W}{\partial x_1} = \frac{\partial W}{\partial \varepsilon_{ij}^m} \frac{\partial \varepsilon_{ij}^m}{\partial x_1} = \sigma_{ij} \frac{\partial \varepsilon_{ij}^m}{\partial x_1} \quad (25)$$

When initial strain is absent, the second term in the above integral is zero. Otherwise,  $\varepsilon_{ij}^m$  is then written as

$$\varepsilon_{ij}^m = \varepsilon_{ij}^e + \varepsilon_{ij}^p + \varepsilon_{ij}^o \quad (26)$$

where,  $\varepsilon_{ij}^e$  and  $\varepsilon_{ij}^p$  are the total elastic and plastic strains, respectively and  $\varepsilon_{ij}^o$  is the initial plastic strain.

Inserting Eqs. (5) and (6) into Eq. (4) lead to a path-independent J-integral definition considering residual stress and initial strain as follows:

$$(J)_{volume} = -\int_v \left( W \frac{\partial q}{\partial x_1} - \sigma_{ij} \frac{\partial u_i}{\partial x_1} \frac{\partial q}{\partial x_j} \right) dV + \int_v \sigma_{ij} \frac{\partial \varepsilon_{ij}^o}{\partial x_1} q dV \quad (27)$$

And  $W$  must be adjusted to account for the initial strain energy density i.e.

$$W = W^{total} - W^P|_{initial}$$

where,  $W^P|_{initial}$  is the plastic work done before the initial state [39]

### 3.2.3 TUBULAR JOINTS (Stress intensity approach)

The accurate evaluation of SIF for surface cracks in tubular joints is a difficult task due to complex geometry of the joint and crack configuration.

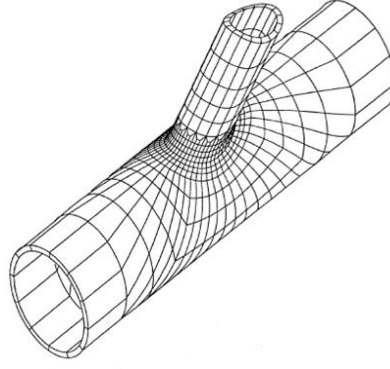


**Fig. 16:** Geometry of Tubular joints [47]

Well established procedures commonly used for evaluating SIF in arbitrary cracked bodies are, displacement extrapolation technique, strain energy release rate (SERR) method and J-integral method. In this paper, displacement extrapolation technique has been used for computing SIF. Bowness and Lee [5] reported an investigation on the prediction of SIF in tubular joints for semi-elliptical surface cracks by using displacement extrapolation technique. The method uses the elastic displacements in the vicinity of the crack front for computing SIF. For the case of plane strain conditions at crack front, the displacement fields are expressed as: [4]

$$\begin{aligned}
 v_n &= \frac{K_I}{G} \sqrt{\frac{r}{2\pi}} \sin \frac{\theta}{2} \left[ 2 - 2\nu - \cos^2 \left( \frac{\theta}{2} \right) \right] \\
 \text{Mode I: } u_r &= \frac{K_I}{G} \sqrt{\frac{r}{2\pi}} \sin \frac{\theta}{2} \left[ 1 - 2\nu + \sin^2 \left( \frac{\theta}{2} \right) \right] \\
 w_t &= 0
 \end{aligned} \tag{28}$$

$$\begin{aligned}
 v_n &= \frac{K_{II}}{G} \sqrt{\frac{r}{2\pi}} \sin \frac{\theta}{2} \left[ -1 + 2\nu + \sin^2 \left( \frac{\theta}{2} \right) \right] \\
 \text{Mode II: } u_r &= \frac{K_{II}}{G} \sqrt{\frac{r}{2\pi}} \sin \frac{\theta}{2} \left[ 2 - 2\nu + \cos^2 \left( \frac{\theta}{2} \right) \right] \\
 w_t &= 0
 \end{aligned} \tag{29}$$

$$\begin{aligned}
 v_n &= 0 \\
 \text{Mode II: } u_r &= 0 \\
 w_t &= \frac{K_{III}}{G} \sqrt{\frac{r}{2\pi}} \sin \left( \frac{\theta}{2} \right)
 \end{aligned} \tag{30}$$

where,  $K_I$ ,  $K_{II}$  and  $K_{III}$  are the SIF for Modes I, II and III, respectively;  $G$ , the shear modulus;  $\nu$ , the Poisson's ratio; and  $u_r$ ,  $v_n$  and  $w_t$  denote the local radial, normal and tangential displacements, respectively, as shown in **Fig. 17**. The plane stress form of these equations is obtained by substituting  $\nu$  by  $\nu / (1 + \nu)$

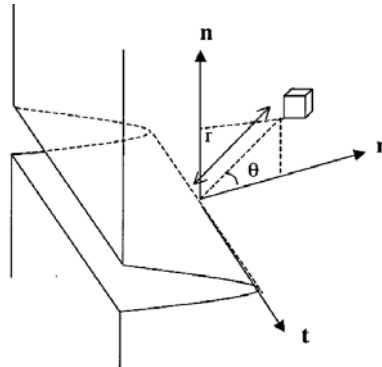


**Fig.17:** Local axes system at crack front [47]

Using the displacements near the crack front obtained from FE analysis, the corresponding SIF may be calculated by using equations (28)-(30). The SIF for a particular radial path are then plotted against the distance from the crack tip. The crack front SIF may then be found by extrapolating the linear part of the distribution back to the crack front. In order to apply the displacement extrapolation technique to a doubly curved crack in a tubular joint, the local radial, normal and tangential directions must be defined for each point on the crack front. This is achieved by first calculating the vectors defining the local directions, which is quite straightforward as the crack is planar and lies in one of the global planes. The radial direction is calculated from the co-ordinates of the nodes on the radial paths along the crack front. The tangential direction is determined from the derivative of the equation defining the elliptical crack front. The two vectors defining these directions are then mapped to vectors defining the local radial and tangential directions for the doubly curved weld toe crack. The third vector in the normal direction is then generated from a cross product of the other two. Having determined these local directions, the global displacements from the FE analysis may then be transformed into local displacements as:

$$\begin{Bmatrix} u_r \\ v_n \\ w_t \end{Bmatrix} = \begin{bmatrix} l_1 m_1 n_1 \\ l_2 m_2 n_2 \\ l_3 m_3 n_3 \end{bmatrix} \begin{Bmatrix} \delta X \\ \delta Y \\ \delta Z \end{Bmatrix}$$

where  $\delta X$ ,  $\delta Y$  and  $\delta Z$  are the global displacements and  $l_1, m_1, n_1$  etc are the direction cosines of the local directions with respect to the global axes X, Y and Z. To evaluate SIF, the largest displacement in the vicinity of the crack, obtained from the radial paths up the crack front, i.e.  $q = \pm 180^\circ$  is generally chosen[48].

## 4. FATIGUE ANALYSIS

### 4.1 FUNDAMENTAL KNOWLEDGE ON FATIGUE ANALYSIS

Fatigue is the progressive and localized structural damage that occurs when a material is subjected to cyclic loading. The maximum stress values are less than the ultimate tensile stress limit, and may be below the yield stress limit of the material. Failure of a material due to fatigue may be viewed on a microscopic level in three steps:

1. **Crack Initiation** - The initial crack occurs in this stage. The crack may be caused by surface scratches caused by handling, or tooling of the material; threads (as in a screw or bolt); slip bands or dislocations intersecting the surface as a result of previous cyclic loading or work hardening.
2. **Crack Propagation** - The crack continues to grow during this stage as a result of continuously applied stresses
3. **Failure** - Failure occurs when the material that has not been affected by the crack cannot withstand the applied stress. This stage happens very quickly.

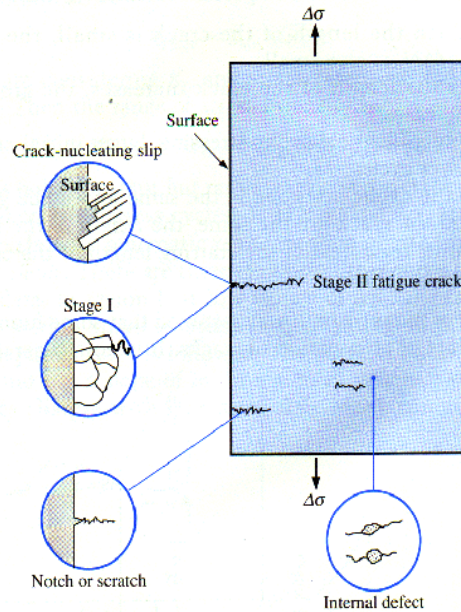


**Fig. 18: Crack Propagation Due to Fatigue** [52]

The **Fig. 18** illustrates the various ways in which cracks are initiated and the stages that occur after they start. This is extremely important since these cracks will ultimately lead to failure of the material if not detected and recognized. The material shown is pulled in tension with a cyclic stress in the y, or horizontal direction. Cracks can be initiated by several different causes. There are several methods for fatigue assessment which are frequently used in fatigue life prediction or fatigue crack propagation of welded structures and components. They can be divided as global approaches- *Nominal* and *Geometric Stress Method* and local approaches- *Effective Notch Stress Method* and *LEFM (Linear Elastic Fracture Mechanics)*. [24] All these methods are described briefly in this paper:

#### 4.1.1 NOMINAL STRESS

Nominal stress can, in simple cases, be calculated analytically using elementary theories of structural mechanics, based on linear-elastic behavior. In general the simple formula can be used:

$$\sigma_{nom} = \frac{F}{M} + \frac{M}{W} \quad (31)$$

### 4.1.2 GEOMETRIC STRESS

The geometric stress (**Fig. 19**) incorporates all the stress raising effects on a structural detail, with the exception of stress concentration originating from the weld itself. In fatigue calculation, the geometric stress must be determined in the critical direction and location on the welded joint. The approach is not appropriate for joints where the crack would develop from the root of the weld or from an internal defect. Geometric stress is calculated by taking the stress provided by the finite element analysis or calculated from the deformation measured by gauges at specified distances from the bead toe, as shown in **Fig. 19b**. The geometric stress at the bead toe is extrapolated from the values obtained at the measuring points using a two- or three-point formula, in accordance with the following equations:

$$\begin{aligned}\sigma_{HS} &= 1.67\sigma_{0.4t} - 0.67\sigma_{1.0t} \\ \sigma_{HS} &= 2.52\sigma_{0.4t} - 2.24\sigma_{0.9t} + 0.72\sigma_{1.4t}\end{aligned}\tag{32}$$

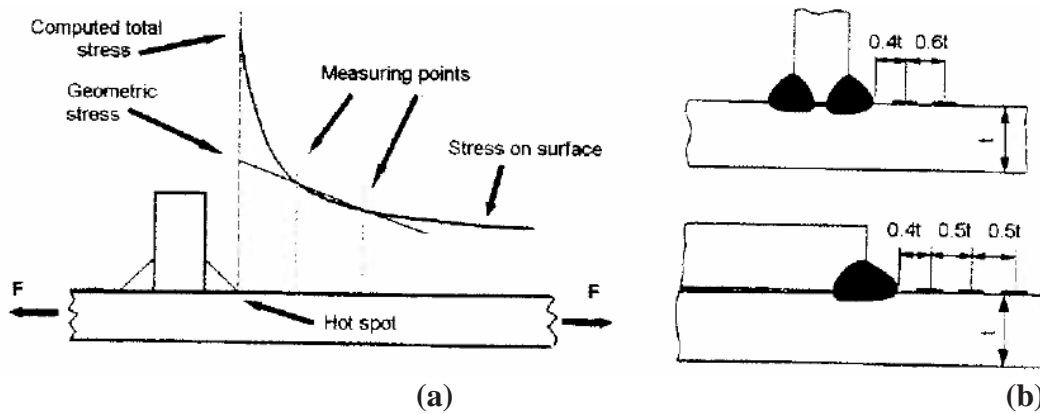


**Fig. 19:** Definition of geometric stress (a) and extrapolation points (b) [25]

### 4.1.3 EFFECTIVE NOTCH STRESS METHOD

The effective notch stress is the maximum stress measured at the notch, corresponding to a radius of 1 mm, as shown in **Fig. 20**, assuming linear elastic behaviour in the material. One essential benefit of this method is that the notch stress is independent of the geometry, so that a common fatigue strength curve can be used.

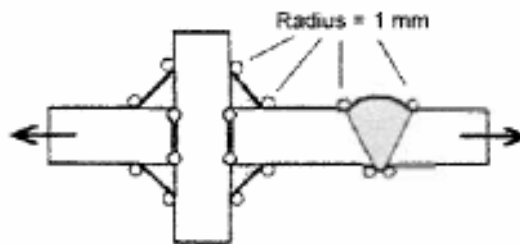


**Fig. 20:** Principle of applying 1 mm notch radius at the bead toe and root [25]

#### 4.1.4 LINEAR ELASTIC FRACTURE MECHANICS

The basic procedure of fracture mechanics used for fatigue crack propagation based on the following two equations:

- fatigue crack growth equation,  $da/dN$  (in m/cycle)

$$\frac{da}{dN} = C(\Delta K)^m \quad (33)$$

- stress intensity factor range,  $\Delta K$  (in  $\text{MPa}\sqrt{\text{m}}$ )

$$\Delta K = F(a)\Delta\sigma\sqrt{\pi a} \quad (34)$$

where,  $a$  = initial crack size in the direction of the crack growth,  $C$ ,  $m$  = material constant,  $\Delta\sigma$  = applied nominal stress,  $F(a)$  = correction factor for the stress intensity factor.

In the literature some engineering values for initial crack sizes in welds in steel can be found. Radaj (50) give the value  $a = 0.1-0.5$  mm for a line crack and for a semi elliptical crack, he give  $a/c = 0.1 - 0.5$  for the depth/width ratio. In a literature survey by Samuelsson (51) the following typical flaw sizes were found for use in conjunction with welds. At the surface, welding causes defects with depths from 0.01 to 0.05 mm.

When the applied stress range,  $\Delta\sigma$ , is constant during crack propagation, fatigue crack growth equation can be written as follows

$$dN = \frac{da}{C[F(a)\Delta\sigma\sqrt{\pi a}]^m} \quad (35)$$

Then, the fatigue crack propagation life,  $N_p$ , from an initial crack size  $a_i$  to a final crack size  $a_f$  can be computed as follows:

$$N_p = \int_{N_i}^{N_f} dN = \int_{a_i}^{a_f} \frac{da}{C[F(a)\Delta\sigma\sqrt{\pi a}]^m} \quad (36)$$

The stress intensity factor range,  $\Delta K$ , for a crack initiating at the weld toe may conveniently express as follows:

$$\Delta K = F_S \cdot F_E \cdot F_G \cdot F_T \cdot \sigma \sqrt{\pi a} \quad (37)$$

where,  $F_S$  = correction factor for free surface,  $F_E$  = correction factor for crack shape,  $F_G$  = geometry correction factor accounting for the effect of stress concentration due to geometrical discontinuity,  $F_T$  = correction factor for finite thickness or finite width. [46].

## 4.2 WELDED JOINTS ANALYSIS BASED ON FATIGUE ANALYSIS

### 4.2.1 BUTT JOINT (Theoretical Model)

The process of the fatigue failure in the welded joints can be divided into two main periods: micro cracks nucleation, growth and coalescence (stage I fatigue crack) and macro crack propagation to a length, which causes fracture (stage II fatigue crack). The boundaries of the periods are poorly defined, but it is useful to think that the total fatigue life  $N_F$  consist of macro crack initiation period  $N_I$  and macro crack propagation period  $N_P$ :

$$N_F = N_I + N_P \quad (38)$$

Macro crack initiation S- $N_I$  curve can be now written on the basis of the fatigue strength on  $N=500$  load cycles  $\Delta\sigma_{500}$  and fatigue strength on  $N=2 \cdot 10^6$  load cycles  $\Delta\sigma_E$ :

$$N_I = \left( \frac{\Delta S \cdot K_f}{\Delta\sigma_E} \right) \cdot 2 \cdot 10^6 \quad (39)$$

where,  $\Delta S$  is nominal stress range. The slope of S- $N_I$  curve  $m_I$  is

$$m_I = \frac{\log(2 \cdot 10^6) - \log(500)}{\log\left(\frac{\Delta\sigma_E}{K_f}\right) - \log(\Delta\sigma_{500})} \quad (40)$$

The material fatigue strength,  $\Delta\sigma_{500}$  and  $\Delta\sigma_E$  can be estimated using Basquin-Morrow equation:

$$\begin{aligned} \Delta\sigma_{500} &= 2 \cdot (\sigma_f' - \sigma_m) \cdot 500^b \\ \Delta\sigma_E &= 2 \cdot (\sigma_f' - \sigma_m) \cdot 2 \cdot 10^6^b \end{aligned} \quad (41)$$

where  $\sigma_m$  is the mean stress,  $\sigma_f'$  is fatigue-strength coefficient and  $b$  is fatigue-strength exponent. The fatigue strength parameters can be determined most accurately by experimental testing. The testing of a narrow HAZ zones is very difficult or impossible. Alternative, the fatigue strength parameters can be estimated from the material tensile properties or hardness values. Lawrence et al (1981) purposed the Brinell hardness based estimation for steel with hardness between 150 HB and 700 HB:

$$\sigma_f' \approx 3.42 \cdot HB + 342 \text{ MPa} \quad (42)$$

$$b \approx -\frac{1}{6} \log\left(\frac{2 \cdot (HB + 100)}{HB}\right)$$

The relationship between the Brinell hardness HB and Vickers hardness HV can be carried out using the conversion table from Metals handbook (Boyer and Gall, 1985):

$$HB \approx 0.98HV^{0.994} \quad (43)$$

A reduction of fatigue strength by notch i.e. fatigue notch factor can be calculated using Peterson's equation:

$$K_f = 1 + \frac{K_t - 1}{1 + \frac{a_p}{\rho}} \quad (44)$$

where,  $K_t$  is elastic stress concentration factor,  $\rho$  is notch root radius and  $a_p$  is Peterson's material parameter relating to the material ultimate strength (Peterson, 1974). The notch radius is determined so that  $K_f$  gets the maximum value using analytical formulations developed for butt welds (Anthes et al., 1994). The ultimate strength for a narrow HAZ is estimated from material hardness value HV (Boyer and Gall, 1985).

Hardness based estimation for steel is:

$$S_u \approx 3.074HV - 25 \quad HV \leq 340 \quad (45)$$

The advantage of the approach is that S-N curve for macro crack initiation can be calculated from the material hardness at the macro crack initiation point i.e. weld root or toe.

Macro crack propagation period is calculated using the Paris Law and the propagation equation by Forman et al. (1967):

$$N_p = \int_{a_i}^{a_c} \frac{1-R}{C\Delta K^n} da \quad (46)$$

Where,  $\Delta K$  is the stress intensity factor,  $a_i$  is the initiated crack size,  $a_c$  critical crack length and C, n are material constants.

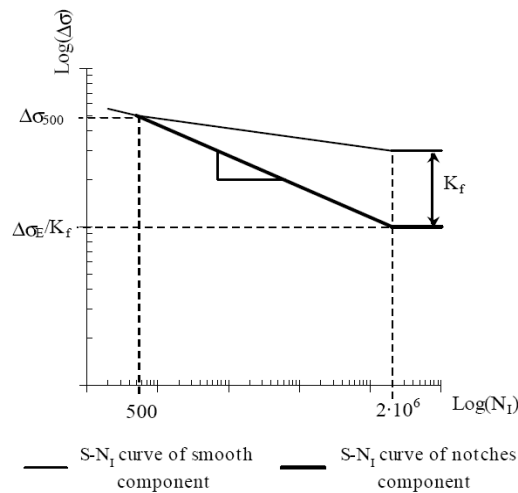


**Fig. 21:** Schematic presentation for determination of S-N<sub>I</sub> curve for notched component [11]



## 4.2.2 LAP JOINT (Static Stress and Local Stress-Strain Analysis)

### Static Stress Analysis

An idealized lap joint configuration is employed in the analysis (**Fig.22**). The overlap length ( $2c$ ), the sheet thickness ( $t$ ), and the interlayer gap width ( $\eta$ ) are the three essential geometric variables. The local stresses at the sheet-to-sheet interface are assumed to be in a state of plane strain because the sheet width is very large compared to either the sheet thickness or the gap width.

In order to analyse the stresses at the lap joint interface, it is necessary to determine the loading that must be transmitted through the joint. These loads consist of a tension,  $T$ , a moment,  $M_0$ , and a shearing force,  $V_0$ , each per unit of joint width (**Fig. 22**).

The critical location for failure initiation is most often at the edge of the interlayer. Thus employing the Von Mises distortion energy criterion to give a combined stress parameter,  $J$ , given by:

$$J = (\sigma_y^2 + \tau_{xy}^2)^{1/2} \quad (47)$$

The failure stress concentration,  $J/P$  ( $P$  being the normal stress in the sheet away from the joint) is thus considered to be the theoretical stress concentration factor (TSCF),  $K_t$ .

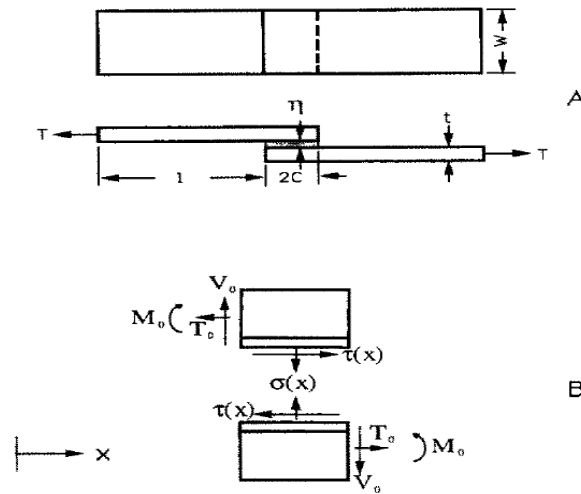


**Fig 22:** Loads and symbol definition of joint: A-Joint dimensions and end load, B- Resolved loads and stresses at joint ends and mid plate [23]

### Local Stress-Strain Analysis

During fatigue testing the local stress amplitude at the joint interface is higher than the stress in the sheet away from the joint due to stress concentration effects. Conventionally the nominal stress in the sheet is plotted against cycles to failure in developing S-N curves. Local stress concentrations thus decrease the observed fatigue strength. The stress concentration is so severe with welded lap joints that the observed fatigue strength is very low using this technique.

The concept of local stress-strain behaviour has been developed to account for geometric stress concentration effects.

$$\sigma_a \left[ \frac{\sigma_a}{E} + \left( \frac{\sigma_a}{\sigma'_f} \right)^{1/n'} \right] = \frac{(K_t S_a)^2}{E} \quad (48)$$

where,

$\sigma_a$  = local stress amplitude,  $E$  = Young's Modulus,  $\sigma'_f$  = fatigue strength co-efficient,  $n'$  = fatigue strain hardening exponent,  $S_a$  = nominal stress amplitude,  $K_t$  = theoretical concentration factor.

Combining above two equations allows one to calculate a stress or a stress concentration under static loading at the critical location at the edge of the layer between sheets, and then to modify this stress level for fatigue loading conditions. The combined model thus provides a prediction of welded lap joint behaviour from smooth sheet fatigue data. [23]

## 5. MULTI-SCALE MODELLING

In every day engineering, many failures are due to the pre-existence of various types of defects in the material's micro-scale [53]. The propagation and coalescence of micro cracks, micro voids and similar defects in the micro-scale leads eventually to the complete rapture of the component [54]. One of the principal objectives of micro/nanomechanics of materials is to account for the observed phenomena and properties of macroscopic solid bodies, such as strength and fracture toughness of metals, on the basis of the quantum mechanical theory of the behaviour of atomic particles. Success will have been achieved when it becomes possible to calculate the quantities that describe the constitution of materials and their response to alterations of macroscopic mechanical boundary conditions from the knowledge of the component elements and their hierarchical structures from atomistic–electronic scales to micro- and macro scales [55]. Therefore, it is seen that there is a need for modelling materials in different scales and actually monitoring their behaviour simultaneously.

### 5.1 Multi-scale approaches

A series of different multi-scale approaches have been established, however only some of them for high strength steel. Multi-scale approaches introduced modelling at the mesoscale, like the Cellular Automation model or the Monte Carlo Potts model. These approaches are particularly suitable for welding and hot forming processes, as they consider the recrystallization process by adding small embryos with new re-orientation, provided the local net energy is reduced [56]. As an alternative to FEA, the Boundary Element Method is meanwhile established for multi-scale modelling, particularly for fracture problems, as it reduces the dimensionality and thus the computation time/storage. E.g. for  $Al_2O_3$ -cracking a multi-scale model was developed [55] by employing a fully frictional contact analysis (contacting, sliding, sticking, separation) at the grain scale, allowing at the macro-scale for multiple intergranular crack initiation and propagation under mixed-mode failure conditions, **Fig. 23**.

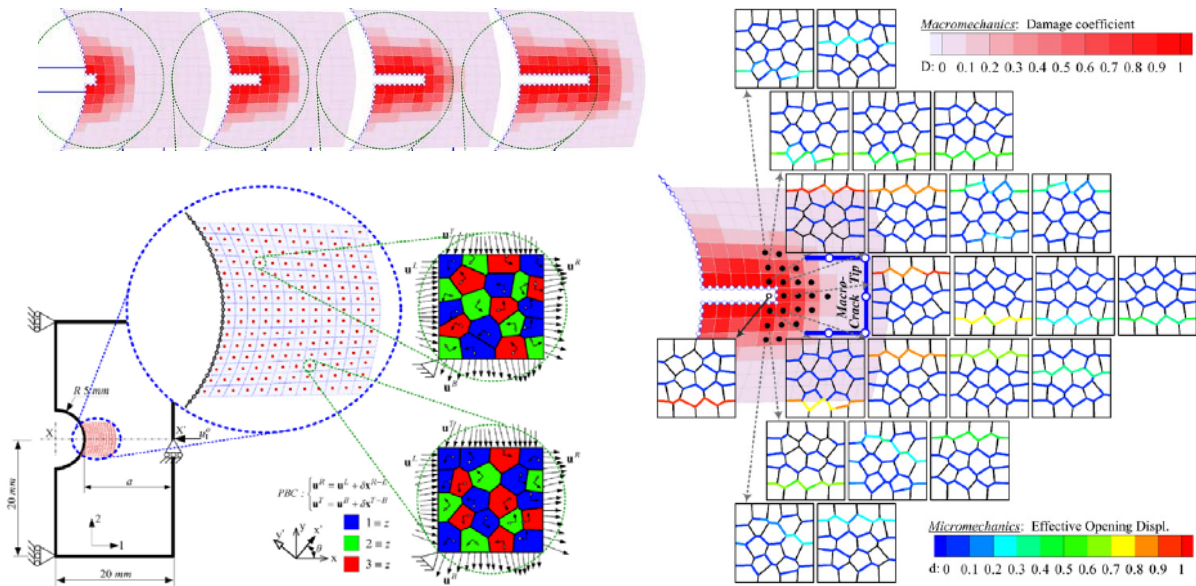


**Fig. 23:** Multi-scale model for crack propagation: stress formation in the macro scale (upper left), average properties mesoscale (right), RVE grain scale (lower left) [55]

### 5.1.1 Macro continuum scale

Finite Element simulation of the stress formation and the strain response of a weld under load conditions is a common method often applied at the macro continuum scale. The difficulties are meshing at locations with small dimensions/curvatures or strong deformations. Moreover, valid material properties are needed, often by empirically identified material models. For single phase metals the stress-strain curve is often developed by an empirical model based on the chemical composition, while modelling of the physics is based on the density of dislocations and mobility of the grain boundaries.

However, for multi phase materials like high strength steels (DP, TRIP) and for the different zones of a weld the identification is difficult as the micro polycrystal structure is heterogeneous, which demands for modelling of the material properties at one or several micro-scale levels.

### 5.1.2 Microstructure and RVE-scale

A recently often applied method for modelling the formability at the micro-scale is the Representative Volume Element (RVE) method for solving the crystal plasticity constitutive equations. The RVE can be determined by SEM-EBSD measurement. **Fig. 24** shows the different phases of an RVE model

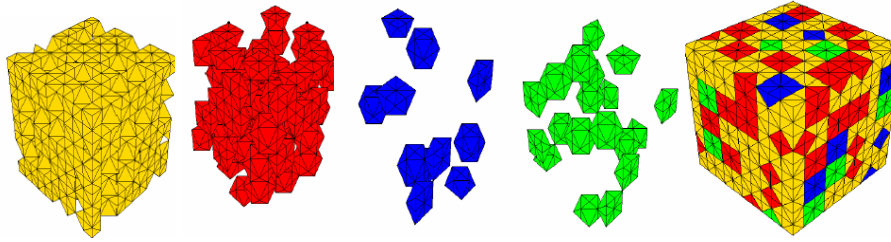


**Fig. 24:** Four phases (ferrite, bainite, retained austenite, martensite) of the RVE (cube size e.g. of the order of 100  $\mu\text{m}$ ) of a TRIP steel

Many RVE models have been developed, but they suffer from lack of describing the grain location, size or orientation accurately in 3D space, due to the strong interaction with adjacent grains to be considered.

### 5.1.3 Crystallic/atomic scale

Both, plastic deformation and fracture have their origin at the atomic scale. While deformation is caused by the propagation of dislocations (atomistic sliding), governed by the Rice criterion, during fracture of a crystal atomic aggregates are split into two parts, as can be calculated by a universal relation for the binding energy leading to a newly created surface energy. The imperfections of real crystals have to be taken into account, such as impurity or interstitial atoms, vacant lattice site and dislocations. Calculation of these lattice-particle interactions at the atomic level is complicated, but essential for understanding and control of separation or dislocation propagation, as it is the key for setting goals for the development of advanced high strength steel types.

## 6. WELDING STANDARD

Welding standard in Hybrid laser welding is not prepared yet by any international organization. The available welding standards are ISO 5817 (Welding-Fusion welded joints in steel, nickel, titanium and their alloys-Quality levels of imperfections), ISO 9692-1 (Welding and allied processes- recommendations for joint preparation, BS EN ISO 6520-2 (Welding and allied processes- Classification of geometric imperfections in metallic materials - Welding with pressure) etc. Therefore separate standards, based on existing welding standards, have to be prepared.

## 7. CONCLUSION

- Finite element modelling is a powerful method for calculating fracture and fatigue of welded joints.
- ANSYS and ABAQUS are widely accepted commercial simulation software.
- Stress intensity factor (K) is one of the most important parameter in fracture mechanics for the mathematical model of welded joints.

- Recent trends of fracture research include dynamic and time-dependent fracture on nonlinear materials, fracture mechanics of microstructures, and models related to local, global, and geometry-dependent fractures.
- LEFM is capable to describe crack growth and crack propagation in welded structures in a physically correct way.
- An engineering value of initial crack size at weld toe would be 0.1 mm.
- From the publication survey, it can be said that the critical weld location is at the toe for different joint.
- More research effort is required on hybrid laser welded joints.

## 8. ACKNOWLEDGEMENTS

The authors are grateful to VINNOVA – The Swedish Innovation Agency (project HYBRIGHT, no. 27382-2) for funding the research.

## 9. LITERATURE

1. Jaroslav M, *Finite element analysis and simulation of welding – an addendum: a bibliography (1996-2001)*, Modelling Simul. Mater. Sci. Eng., Vol. 10, pp. 295-318 (2002).
2. [http://www.efunda.com/formulae/solid\\_mechanics/fracture\\_mechanics/fm\\_intro.cfm](http://www.efunda.com/formulae/solid_mechanics/fracture_mechanics/fm_intro.cfm)
3. O’Dowd N P, Nikbin K M, Lee H-Y, Wimpory R, Biglari F, *Stress intensity factors due to residual stresses in T-plate welds*, J. Press Vessel Technol, pp.6-12 (2004).
4. Anderson T L, *Fracture Mechanics fundamentals and applications*, ISBN 0-8493-4260-0.
5. Bowness D, Lee M M K, *A finite element study of stress fields and stress intensity factors in tubular joints*, Journal of Strain Analysis, Vol. 30, pp. 135-142 (1995).
6. HSU C, Albright C E, *Fatigue analysis of laser welded lap joints*, *Engineering Fracture Mechanics*, Vol. 39, No. 3, pp. 575-580 (1991).
7. Baohua C, Yaown S, Liangqing L, *Studies on the stress distribution and fatigue behaviour of weld-bonded lap shear joints*, Journal of Materials Processing Technology, pp. 307-313 (2001).
8. Dong P, *A structural stress definition and numerical implementation for fatigue analysis of welded joints*, International Journal of Fatigue, Vol. 23, pp. 865-876, (2001).
9. El-Sayed M E M, Stawiarski T, Frutiger R, *Fatigue analysis of spot-welded joints under variable amplitude load history*, Engineering Fracture Mechanics, Vol. 55, No. 3, pp. 363-369 (1996).

10. Henrysson H F, **Fatigue life predictions of spot welds using coarse FE meshes**, Fatigue Fracture Engineering Material Structure, Vol. 23, pp. 737-746 (2000).
11. Remes H, **A theoretical model to predict fatigue life of laser welded joints**, Ship laboratory, Helsinki University of Technology, Finland.
12. Cho S K, Yang Y S, Son K J, Kim J Y, **Fatigue strength in laser welding of the lap joint**, Finite Elements in Analysis and Design, Vol. 40, pp. 1059-1070 (2004).
13. Maddox S J, **An analysis of fatigue cracks in fillet welded joints**, International Journal of Fracture, Vol. 11, No. 2, pp. 221-243 (1975).
14. Alam M S, Wahab M A, **Modeling the fatigue crack growth and propagation life of a joint of two elastic materials using interface elements**, International journals of pressure vessels and piping, Vol. 82, pp. 105-113 (2005).
15. Etube L S, Bremen F P, Dover W D, **A new method for predicting stress intensity factors in cracked welded tubular joints**, International Journal of Fatigue, Vol. 22, pp. 447-456 (2000).
16. Sutton M A, Reynolds A P, Ge Y Z, Deng X, **Limited weld residual stress measurements in fatigue crack propagation: Part II FEM based fatigue crack propagation with complete residual stress fields**, Fatigue Fracture Engineering Material Structure, Vol. 29, pp. 537-545 (2006).
17. Balasubramanian V, Guha B, **Effect of weld size on fatigue crack growth behaviour of cruciform joints by strain energy density factor approach**, Theoretical and Applied Fracture Mechanics, Vol. 31, pp. 141-148 (1999).
18. Haagensen P J, Statnikov E S, Martinez L L, **Introductory fatigue tests on welded joints in high strength steel and aluminium improved by various methods including ultrasonic impact treatment**, IIW Doc. XIII- 1748-98.
19. Teng T L, Chang P H, **Effect of residual stresses in fatigue crack initiation life for butt-welded joints**, Journal of Materials Processing Technology Vol. 145, pp. 325-335 (2004).
20. Li X Y, Partanen T, Nykänen T, Björk T, **Finite element analysis of the effect of weld geometry and local condition on fatigue strength of lap joint**, International Journal of Pressure Vessels and Piping, Vol. 78, pp. 591-597 (2001).
21. Ding F, Zhao T, Jiang Y, **A study of fatigue crack growth with changing loading direction**, Engineering Fracture Mechanics, Vol. 74, pp. 2014-2029 (2007).
22. Caccese V, Blomquist P A, Berube K A, **Effect of weld geometric profile on fatigue life of cruciform welds made by laser/GMAW processes**, Marine Structures, Vol. 19, pp. 1-22 (2006).

23. Hsu C, Albright C E, **Fatigue analysis of laser welded lap joints**, Engineering Fracture Mechanics Vol. 39, No. 3, pp. 575-580 (1991)
24. Barsoum Z, **Residual Stress Analysis and fatigue of Welded Structures**, Licentiate Thesis, Dept. of Aeronautical and Vehicle Engineering, KTH, Sweden 2006. ISBN 91-7178-264-8
25. Pettersson G, **Fatigue assessment of welded structures with non-linear boundary conditions**, Licentiate Thesis, Dept. of Aeronautical and Vehicle Engineering, KTH, Sweden 2004. ISBN 91-7283-948-1.
26. Andersson P, Segle P, Samuelson L Å, **Numerical investigation of creep crack growth in cross-weld CT specimens. Part II: influence of specimen size**, Fatigue Fract. Engng. Struct. Vol. 23, pp. 533-540 (1999).
27. Assire A, Michel B, Raous M, **Creep crack initiation and creep crack growth assessments in welded structures**, Nuclear Engineering and Design, Vol. 206, pp. 45-56 (2001).
28. Hou Y C, Pan J, **A fracture parameter for welded structures with residual stresses**, Computational Mechanics, Vol. 22, pp. 281-288 (1998).
29. Infante V, Branco C M, Baptista R, Gomes E, **A residual stresses and fracture mechanics analysis of welded joints repaired by hammer peening**, 8<sup>th</sup> Portuguese Conference on Fracture (2002).
30. Ferreira J M, Pereira A H, Branco C M, **A fracture mechanics based fatigue life prediction for welded joints of square tubes**, Thin Walled Structures, Vol. 21, pp. 107-120 (1995).
31. Cam G, Erim S, Yeni C, Kocak M, **Determination of mechanical and fracture properties of laser beam welded steel joints**, Welding Research Supplement (1999).
32. Atzori B, Lazzarin P, Tovo R, **From a local stress approach to fracture mechanics: a comprehensive evaluation of the fatigue strength of welded joints**, Fatigue Fract. Engng. Struct., Vol. 22, pp. 369-381 (1998)
33. Budden P J, Curbishley I, **Assessment of creep crack growth in dissimilar metal welds**, Nuclear Engineering and Design, Vol. 197, pp. 13-23 (2000).
34. Wang P C, **Fracture mechanics parameter for the fatigue resistance of laser welds**, International Journal of Fatigue, Vol. 17, No. 1, pp. 25-34 (1995).
35. Maosheng C, Shan W, Shaofu L, **Crack growth and fatigue life estimation in welded T- Tubular joints based on fracture mechanics**, Proceedings of the International Offshore Mechanics and Arctic Engineering symposium, Vol. 3, pp. 351-358, (1990).

36. Lieurade H P, **Application of fracture mechanics to the fatigue of welded structures**, *Welding in the world*, Vol. 21, No. 11, pp. 272-295, (1983).
37. Zaho W, Newman J C, Sutton M A, Shivkumar K N, Wu X R, **Stress intensity factors for surface cracks at a hole by a three dimensional weight function method with stresses from the finite element method**, *Fatigue & fracture of engineering materials and structures*, Vol. 21, pp. 229-239 (1996).
38. Schindler H J, Martens H J, Sönnichsen S, **A fracture mechanics approach to estimate the fatigue endurance of welded t-joints including residual stress effects**, *Fatigue Fract. Engng. Mater. Struct.*, Vol. 30, pp. 206-213 (2006).
39. Chang K H, Lee C H, **Residual stresses and fracture mechanics analysis of a crack in welds of high strength steels**, *Engineering Fracture Mechanics*, Vol. 74, Issue 6, pp 980-994 (2007).
40. Lei Y, Dowd N P, Webster G A, **Fracture mechanics analysis of a crack in a residual stress field**, *International Journal of Fracture*, Vol. 106, pp. 195-216 (2000).
41. Lee H Y, Nikbin K M, Dowd N P, **A generic approach for a linear elastic fracture mechanics analysis of a components containing residual stress**, *Int. Journal of Pressure Vessels and Piping*, Vol. 82, pp. 797-806 (2005).
42. Muller W, Veith H, **Influence of weld material properties on fracture mechanics parameters in welds analysed by FEM calculations**, *Int. J. Pres. Ves. & Piping*, Vol. 33, pp. 285-300 (1988)
43. Dahl W, Ehrhardt H, Heuser A, Hubo R, Twickler R, Uwer D, **Determination of fracture mechanics properties of welded joints and comparison with the failure behaviour of wide plates**, *Nuclear Engineering. and Design* Vol. 102, pp. 451-461 (1987).
44. Chiesa M, Skallerud B, Thaulow C, **Fracture analysis of strength-mismatched welded wide plates by line spring elements**, *Engineering Fracture Mechanics*, Vol. 68, pp. 987-1001 (2001).
45. Nykänen T, Li X, Björk T, Marquis G, **A parametric fracture mechanics study of welded joints with toe cracks and lack of penetration**, *Engineering Fracture Mechanics*, Vol. 72, pp. 1580-1609 (2005).
46. Ellyin F, **Fatigue damage, crack growth and life prediction**, ISBN 0-412-59600-8.
47. Cao J J, Yang G J, Packer J A, Burdekin F M, **Crack modelling in FE analysis of circular tubular joints**, *Engineering Fracture Mechanics*, Vol. 61, pp. 537-553 (1998)
48. Murthy A R C, Palani G S, Iyer N R, Appa Rao T V S R, **An efficient FE modelling strategy for fracture analysis of tubular joints**, Vol. 85, pp. 17-51 (2004).



49. <http://www.mpmtechnologies.com/Finite-Element-Fracture-Mechanics.htm>.
50. Radaj D, **Design and analysis of fatigue resistant welded structures**, Abington Publishing (1990), ISBN 1 85573 004 9.
51. Samuelsson J, **Fatigue design of vehicle components: methodology and applications, report 88-23**, Dep. Of Aeronautical Structures and Materials, The Royal Institute of Technology, Stockholm (1998).
52. [http://www.sv.vt.edu/classes/MSE2094\\_NoteBook/97ClassProj/anal/kelly/fatigue.html](http://www.sv.vt.edu/classes/MSE2094_NoteBook/97ClassProj/anal/kelly/fatigue.html).
53. Gagg C R, **Failure of components and products by ‘engineered-in’ defects: case studies**, *Engrg. Fail. Anal.*, pp. 1000–1026 (2000).
54. Scutti J J, McBrine W J, **Failure Analysis and Prevention**, in: W.T. Becker, R.J. Shipley (Eds.), *ASM Handbook*, vol. 11, ASM, USA (2002).
55. Hao S, Liu W K, Moran B, Vernerey F, Olson G B, **Multi-scale constitutive model and computational framework for the design of ultra-high strength high toughness steels**, *Comput. Meth. Appl. Mech. Eng.*, v 193, pp 1865-1908 (2004).
56. Yu Q, Esche S K, **A multi-scale approach for microstructural prediction in thermomechanical processing of metals**, *J Mat Proc Tech*, v 169, pp 493-502 (2005).